iScience

CellPress
OPEN ACCESS

Article

Pathogenic selection promotes adaptive immune variations against serious bottlenecks in early invasions of bullfrogs

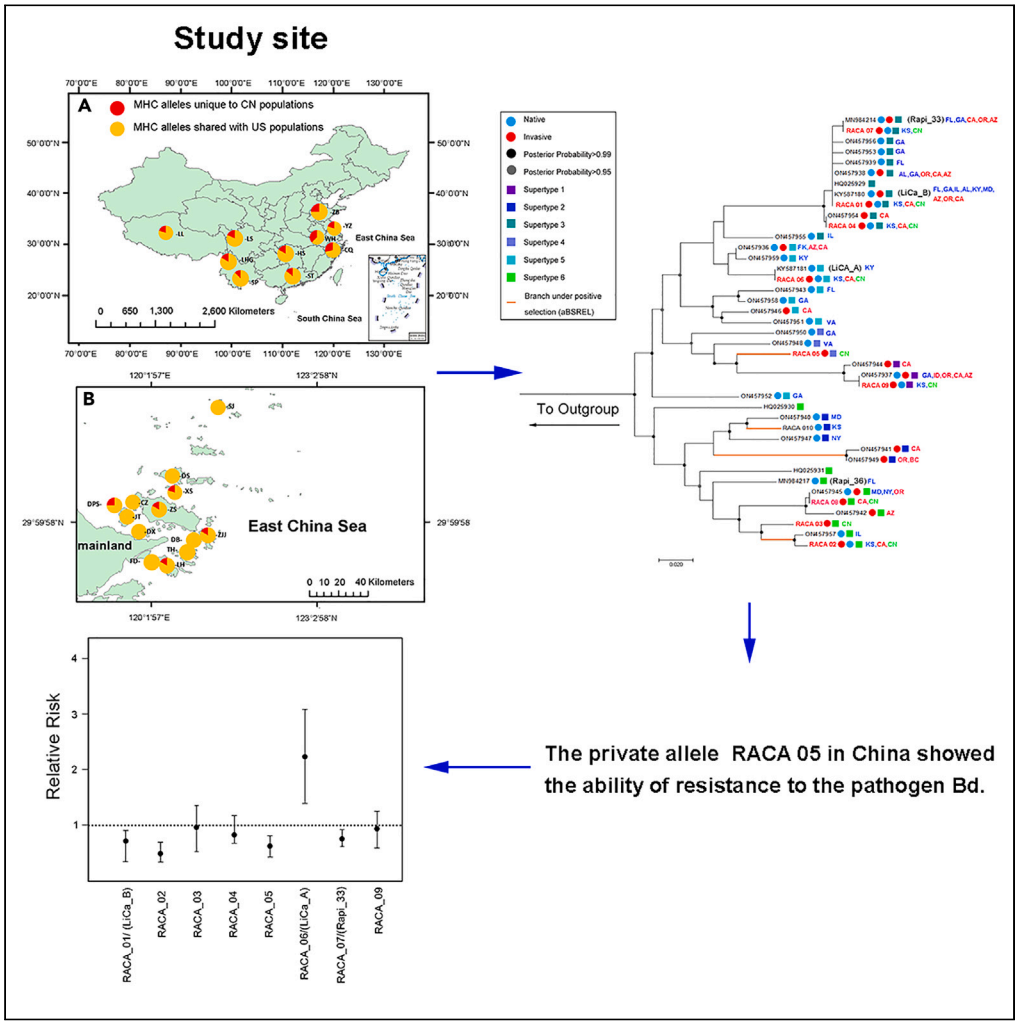

Jiaqi Zhang, Supen Wang, Chunxia Xu, ..., Meiling Niu, Jiaxue Yang, Yiming Li

liym@ioz.ac.cn

Highlights

Adaptive variations are key for understanding evolutionary process affecting invasions

Chinese invasive bullfrogs decrease by 60% in neutral variations vs. US native ones

There are similar variations in immune MHC class-II β gene between China and US

Selection favors MHC variations against bottlenecks in the early invasion of bullfrogs

Zhang et al., iScience 26, 107316
August 18, 2023
https://doi.org/10.1016/j.isci.2023.107316

iScience

CellPress
OPEN ACCESS

Article

Pathogenic selection promotes adaptive immune variations against serious bottlenecks in early invasions of bullfrogs

Jiaqi Zhang,[1,2,5] Supen Wang,[1,4,5] Chunxia Xu,[1,2] Siqi Wang,[1,2] Jiacong Du,[3] Meiling Niu,[3] Jiaxue Yang,[3] and Yiming Li[1,2,3,6,*]

SUMMARY

Adaptive genetic variations are key for understanding evolutionary processes influencing invasions. However, we have limited knowledge on how adaptive genetic diversity in invasive species responds to new pathogenic environments. Here, we compared variations in immune major histocompatibility complex (MHC) class-II β gene and neutral loci in relation to pathogenic chytrid fungus (*Batrachochytrium dendrobatidis*, Bd) infection across invasive and native populations of American bullfrog between China and United States (US). Chinese invasive populations show a 60% reduction in neutral cytb variations relative to US native populations, and there were similar MHC variation and functional diversity between them. One MHC allele private to China was under recent positive selection and associated with decreased Bd infection, partly explaining the lower Bd prevalence for Chinese populations than for native US populations. These results suggest that pathogen-mediated selection favors adaptive MHC variations and functional diversity maintenance against serious bottlenecks during the early invasions (within 15 generations) of bullfrogs.

INTRODUCTION

Biological invasions have negative impacts on the economy and biodiversity.[1–3] Understanding the evolutionary processes that underpin invasions is crucial for informing long-term biosecurity strategies to manage invasion risks.[4] Invasive populations are often subjected to genetic bottlenecks, genetic drift, or founder effects, and show rapid adaptation to new biotic (e.g., parasite, predation, and competitor pressures) and abiotic (climates and soil) environments over short timescales.[5] The genetic paradox of invasions states that invasive species successfully establish and spread in invaded ranges despite reduced genetic diversity due to genetic bottlenecks.[4] Neutral genetic variations reflect the demographic history of populations, and most studies have shown a reduction in neutral genetic diversity relative to source populations.[5] Adaptive genetic variations promote the survival and adaptive potential of natural populations under environmental change[6,7] and are key for understanding evolutionary processes that influence the establishment and expansion of populations.[4] However, we have limited knowledge on how adaptive genetic diversity and relevant functional diversity respond to new environments faced by alien species in invaded ranges.[8–10]

Major histocompatibility complex (MHC) genes are an ideal model for understanding adaptive evolution.[11,12] MHC is a genomic region that plays crucial roles in jawed vertebrate adaptive immune responses to pathogen infection. MHC genes are characterized by extreme polymorphism and strong signatures of positive selection that promote nonsynonymous mutations.[11,12] Classical MHC genes with high polymorphism encode glycoproteins that bind peptides inside the cell and deliver them to the surface for recognition by T cells and natural killer cells. MHC genes can be divided into two major subfamilies: class I genes, which are responsible for presenting cells expressing viral proteins, or tumor antigens, and class II genes, which correspond to extracellular pathogens, including bacteria and helminths.[13] It is generally hypothesized that MHC diversity is maintained by pathogen-mediated balancing selection through mechanisms including heterozygote advantage and negative frequency-dependent selection and diversifying selection.[14,15] Polymorphic exons of MHC genes commonly include peptide-binding sites (PBS, a highly polymorphic region with an excess of nonsynonymous substitutions that encode MHC functional proteins)

[1]Key Laboratory of Animal Ecology and Conservation Biology, Institute of Zoology, Chinese Academy of Sciences, 1 Beichen West Road, Chaoyang, Beijing 100101, China

[2]University of Chinese Academy of Sciences Beijing 100049, China

[3]School of Life Sciences, Institute of Life Sciences and Green Development, Hebei University, Baoding 071002, China

[4]Present address: College of Life Science, Anhui Normal University, Wuhu 241008, China

[5]These author contributed equally

[6]Lead contact

*Correspondence: liym@ioz.ac.cn

https://doi.org/10.1016/j.isci.2023.107316

and other sites (non-PBS). According to the clusters of similar peptide-binding specificity, MHC alleles can be grouped into functional supertypes,[16] a measurement of MHC functional diversity that is useful for the development of effective vaccines capable of activating the cellular arm of the immune response.[17]

Here, we investigated the genetic diversity of the MHC class-II β gene and neutral loci (cytb and 9 microsatellites) in relation to fungal and virus pathogens across 25 populations (20 individuals/population) of American bullfrog (*Lithobates catesbeianus* = *Rana catesbeiana*) in China (23 invasive populations, including 10 mainland populations and 13 insular populations across 9 provinces) and the United States (US) (California invasive population and Kansas native population), and compared differences in these genes among Chinese invasive, US invasive and native populations based on the data collected in this study and published datasets. The bullfrog is one of the 100 worst invasive alien species in the world.[18] Native to eastern North America, the natural range of bullfrogs extends from the Atlantic Coast, north to Newfoundland, to Oklahoma and Kansas.[19] Bullfrogs have been widely introduced throughout the world and have established populations in many countries, and almost every state (including California) in the US. Bullfrog invasions have caused population declines or local extinctions of some native amphibians and snakes in invaded ranges.[20–22] Compared with the invasions (1900s) in the Western US, bullfrogs invaded China more recently. The frog was first introduced into mainland China in the late 1950s from Cuba as a source of food.[23] Naturalized populations of bullfrogs are derived from escapes from bullfrog farms[24] or deliberate releases for religious purposes.[25] The first feral population was established in the 1960s in Hanshou, Hunan Province,[23] while most populations in China were established after 1980, following the rapid development of the bullfrog farm industry.[22,23,26] Previous work on the mitochondrial cytochrome *b* gene (cytb) identified two haplotypes in 288 samples from 42 invaded sites (288 individuals) in Zhejiang, Sichuan and Yunnan Provinces and 222 captive individuals from 15 provinces across mainland China, suggesting a lack of genetic diversity in both commercial and feral populations due to sequential founding events for bullfrog farms.[23] Bullfrog is a reservoir of chytrid fungus (*Batrachochytrium dendrobatidis*, Bd) that causes amphibian chytridiomycosis[27,28] and is susceptible to *frog virus 3* (*FV3*) and *Ambystoma tigrinum* virus of the genus Ranavirus,[29,30] which can result in mass death in captivity. In the US, MHC allelic variants in amphibians have been found to cf. resistance to chytridiomycosis.[31,32] A recent study identified two common MHC alleles of the MHC class-II β gene associated with a significantly decreased risk of Bd infection in bullfrog populations.[8] In China, functional supertypes of an MHC locus in populations of the native black-spotted pond frog (*Pelophylax nigromaculatus*) were found to be positively correlated with the abundance of specific viruses in the environment (Frog virus 3 and *Ambystoma tigrinum* virus).[33] Whether genetic variations in the MHC class-II β gene in bullfrogs are associated with viral pathogens in the wild remains unknown. The recent invasions of bullfrog populations (most established less than 35 years or 15 generations, except Hansou, Table S1) in China provide a good chance of examining how genetic diversity and functional diversity at the MHC class-II β gene react with pathogenic environments in early invasions at a large scale.

RESULTS

Genetic variations in cytb and microsatellites in China compared with invaded and native ranges in the US

We recovered 6 haplotypes for the cytb gene from 500 samples, covering 2 haplotypes in 23 Chinese invasive populations, 5 in the California population (CA), and 6 in the Kansas population (KS) (Figure 1, Table S2). RCAT_01 and 02 (RCAT= *Rana catesbeiana*) had the largest number of samples (Figure 1A) and were shared by all regions (mainland and island populations, CA and KS). While RCAT_03, 04, and 06 were shared by CA and KS, RCAT_05 was private to KS. RCAT_01 dominated in the mainland population, while RCAT_02 predominated in insular populations. All mainland populations except Chaiqiao (CQ) had two haplotypes, while six insular populations had only one haplotype (Table S2).

Combined with the data from GenBank (see STAR Methods), we obtained 80 haplotypes, including 3 haplotypes in China, 14 in the US invaded range, and 72 in the US native range (Figure 2A). While private haplotypes dominated in the US native range, only one haplotype (JQ241268.1) recovered by Bai and colleagues (2012) was private to China. This haplotype was the sister close to ON457989.1 that was shared with AZ (Arizona) and CA. All haplotypes in China (green), CA (red), and KS (blue) were in young branches (the upper part of the phylogenic tree), indicating the similar origin of these haplotypes.

For the cytb gene, the average number of haplotypes (Na) per population, average haplotype diversity (Hd), and average nucleotide diversity (π) per population in Chinese invasive populations were 1.69

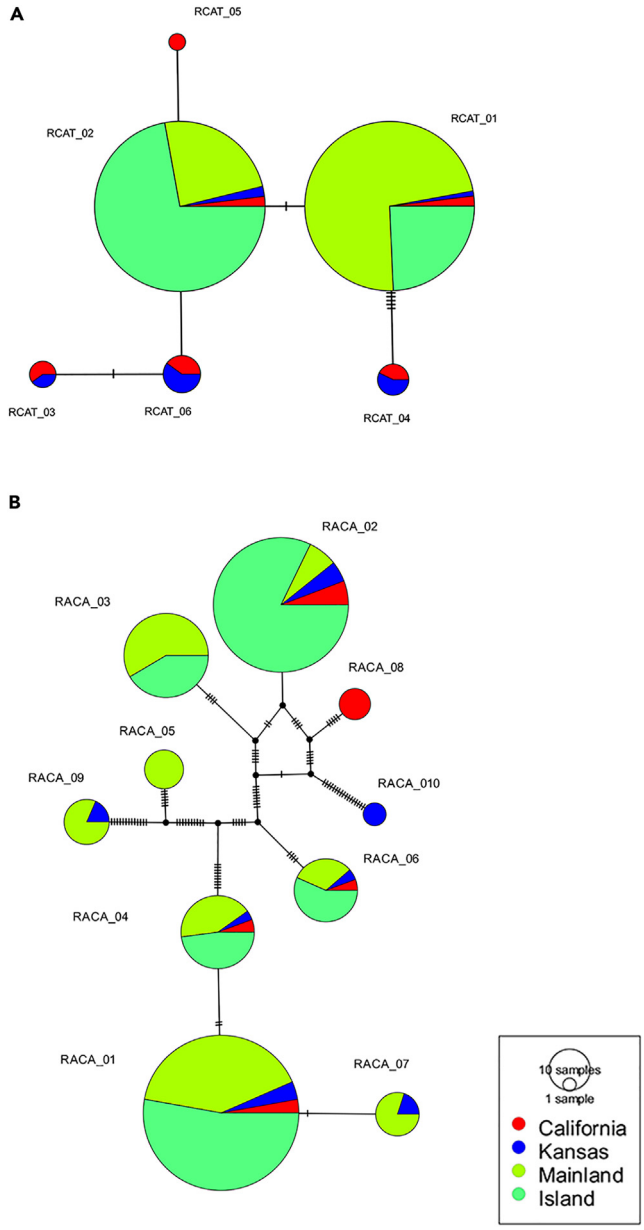

Figure 1. Parsimony network with TCS 95% confidence for cytochrome *b* (cytb) haplotypes and MHC alleles detected across 25 populations of American bullfrogs in this study.Circle size is proportional to the number of individuals

Each line represents a single mutational change, and each mark on the line represents unsampled or extinct haplotypes. (A) cytb; (B) MHC.

haplotypes ±0.47, 0.281 ± 0.217, and 0.00198 ± 0.00322, respectively. Genetic diversity in Chinese invasive populations showed a 61.9% reduction in the number of haplotypes (Mann-Whitney U test, n = 34, $Z = 4.691$, $p < 0.001$, significance level $\alpha = 0.0167$ after Bonferroni correction), 58.7% in Hd ($Z = 3.902$, $p < 0.001$), and 59% in π ($Z = 2.824$, $p = 0.005$) compared with the US native range (11 populations including KS in this study, see STAR Methods) (Figures 3A–3C), and a 39.8% reduction in Na (n = 34, $Z = 2.209$, $p = 0.009$) relative to the US invasive range (11 populations including CA in this study).

The expected heterozygosity (He) and observed heterozygosity (Ho) of 9 microsatellite loci for Chinese populations were 0.69 ± 0.08 and 0.65 ± 0.07, respectively, while He and Ho were 0.72 and 0.64 in CA

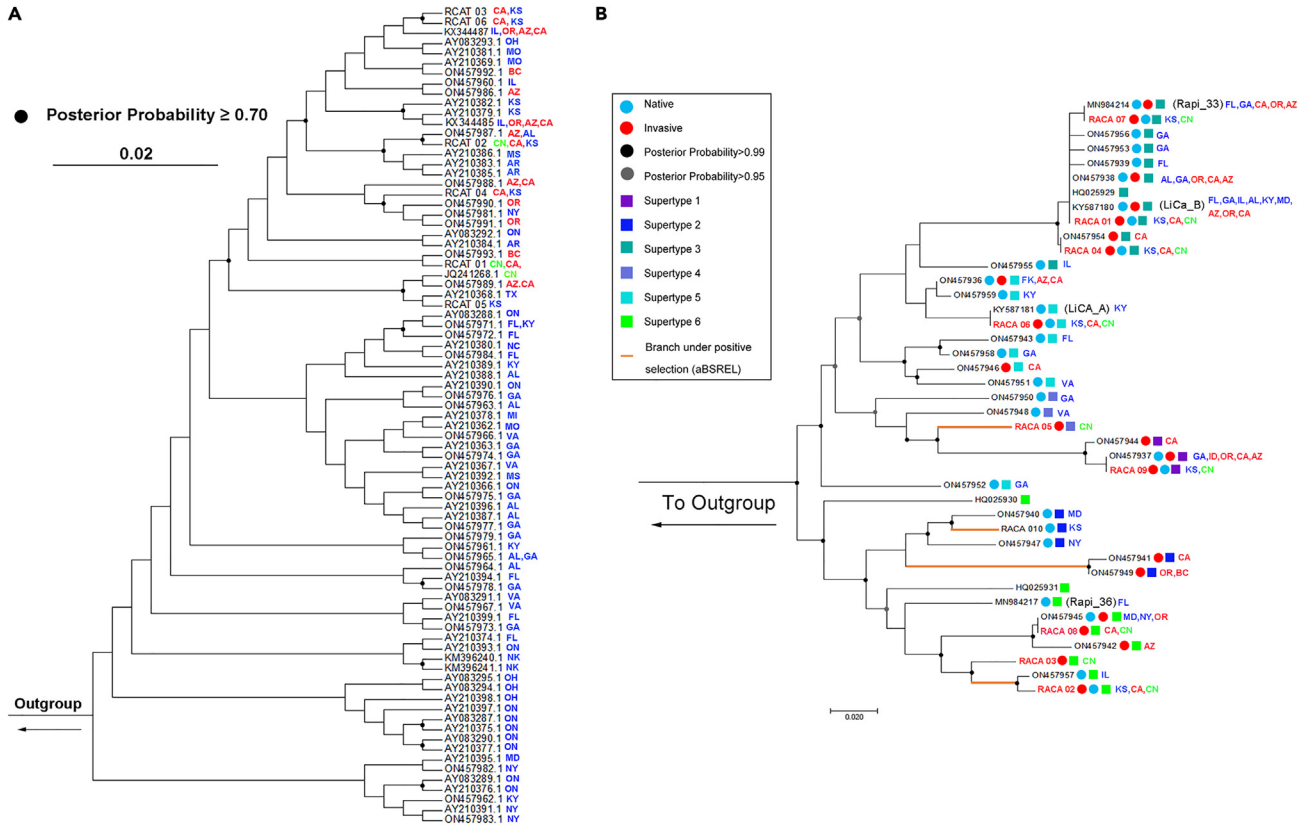

Figure 2. The strict consensus tree from phylogenetic analyses for cytb haplotype genes and MHC alleles or supertypes of bullfrogs using maximum parsimony analysis. RCAT and RACA represent cytb haplotypes and alleles identified in this study, respectively

Codes of other sequences come from NCBI. Acronyms represent sample sites, and CN indicates China.

(A) cytb haplotypes with blue, red and green indicating American native and invaded ranges and Chinese invaded ranges, respectively.

(B) MHC alleles and supertypes.

and 0.67 and 0.56 in KS (Table S3). The mean Na was 5.38 ± 0.89 for the Chinese populations, while the Na for CA and KS were 7.44 and 7.33, respectively. A difference in Na was detected between Chinese populations and two US populations (CA and KS) ($n = 25$, $Z = 2.309$, $p = 0.007$). The Chinese population showed a 27.1% reduction in Na compared to the average value of CA and KS in the US.

Figure 4 shows the population structure of microsatellites for 25 populations (this study) based on allele frequency variation. The populations were grouped into 6 clusters (also see Figure S1): cluster 1 (3 populations: CA, KS, and HS [HS=Hanshou]), cluster 2 (two populations: WH [WH=Wuhu] and LGH [LGH=Luguhu]), cluster 3 (5 populations: ST [ST=Shantou], LL [LL=Lalu], ZB [ZB=Zibo], LS [LS=Liangshan], and SP [SP=Shiping]); cluster 4 (two populations: DPS [DPS=Dapengshan] and FD [FD=Fodu]); cluster 5 (5 populations: CQ, DB [DB=Dengbu], DS [DS=Daishan], XS [XS=Xiushan], and ZJJ [ZJJ=Zhujiajian]); and cluster 6 (4 populations: DX [DX=Daxie], JT [JT=Jintang], SJ [SJ=Sijiao], and TH [TH=Taohua]). The remaining populations (YZ, CZ [CZ=Cezi], LH [Liuheng], and ZS [Zhoushan]) were admixed from different clusters.

MHC diversity and functional supertypes in China compared with those in the US invaded and native ranges

After high-throughput sequencing and filtering (STAR Methods), we identified 10 alleles of the MHC class-II β gene with a length of 272 bp (one locus) (GenBank Accession Numbers: OQ606997–OQ607006) (17 amino acids are located at PBR residues) across 500 individuals (Figure 1B, Table S4; Figure S2), including four new alleles that were first recovered (RACA_02, RACA03, RACA05, and RACA 10) (RACA=*Rana catesbeiana*), six that were recovered previously in *R. catesbeiana*[8,34] (N = 2, Mulder et al. 2017; N = 3, LaFond al.

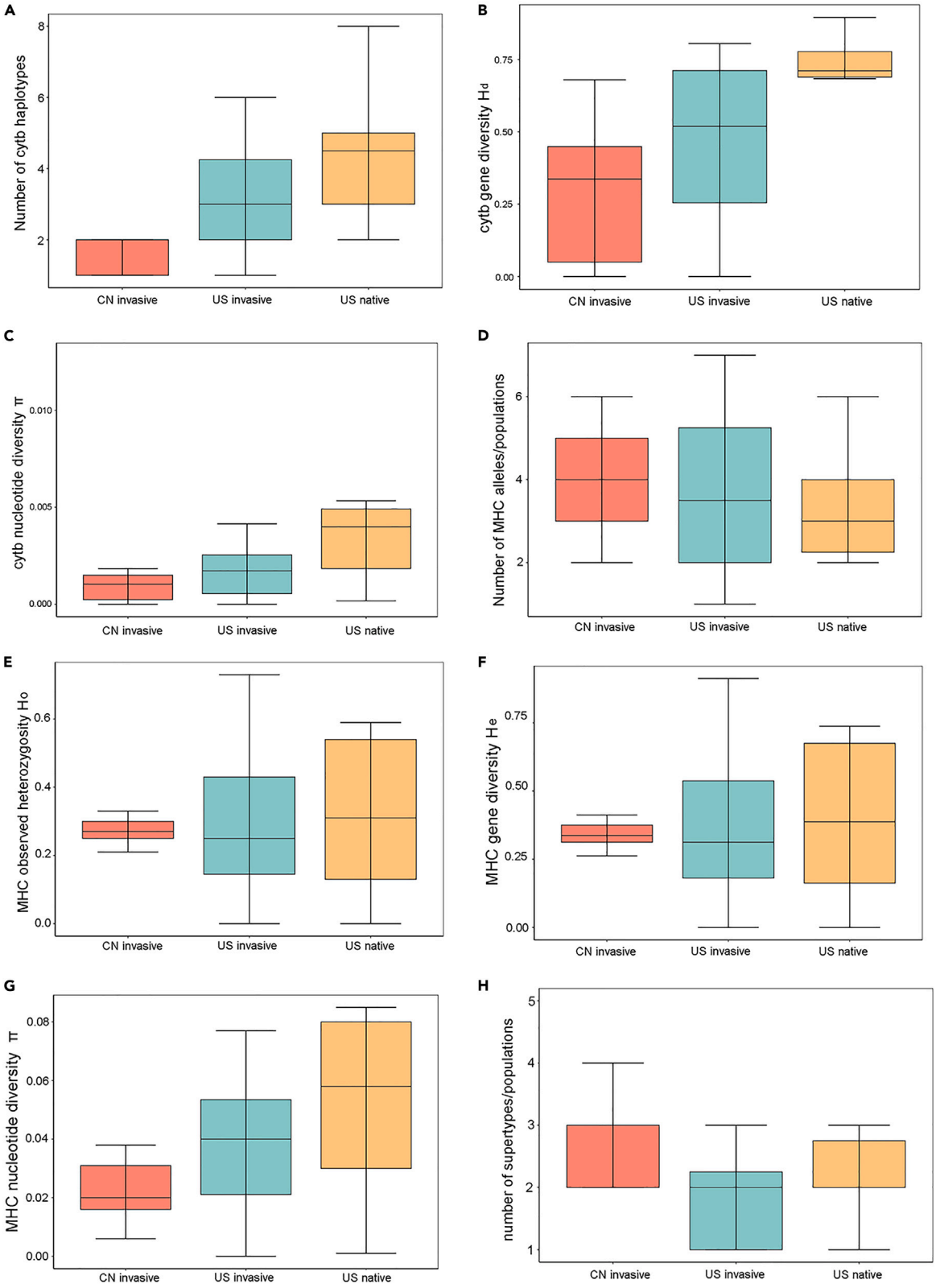
A
Number of cytb haplotypes
8
6
4
2
CN invasive
US invasive
US native
B
cytb gene diversity Hd
0.75
0.50
0.25
0.00
CN invasive
US invasive
US native
C
cytb nucleotide diversity π
0.010
0.005
0.000
CN invasive
US invasive
US native
D
Number of MHC alleles/populations
6
4
2
CN invasive
US invasive
US native
E
MHC observed heterozygosity Ho
0.6
0.4
0.2
0.0
CN invasive
US invasive
US native
F
MHC gene diversity He
0.75
0.50
0.25
0.00
CN invasive
US invasive
US native
G
MHC nucleotide diversity π
0.08
0.06
0.04
0.02
0.00
CN invasive
US invasive
US native
H
number of supertypes/populations
5
4
3
2
1
CN invasive
US invasive
US native

Figure 3. Boxplots of cytb diversity, MHC diversity, and supertypes for bullfrogs among Chinese invasive populations and American native and invasive populations

(A– C) represent the number of haplotypes, Hd and π for the cytb gene, respectively.

(D– G) represent alleles Ho, He, and π for the MHC gene.

(H) Indicate MHC supertypes. (Error bars represent confidence intervals.).

2022), and *R. pipiens*[35] (N = 1; Trujillo et al. 2021). RACA_01 and RACA_02 had the largest number of samples. RACA_04 and 06 were shared by all regions, while RACA_07 and 09 were shared with Chinese mainland populations and KS. Chinese populations carried an average of 3.65 $\pm$ 1.00 MHC alleles, ranging from a minimum of 2 alleles in CZ, DPS, and SJ to a maximum of 6 alleles in AH (AH=Anhui). The CA and KS populations carried 5 and 7 alleles, respectively.

Combining those from GenBank[8] (Accession Numbers: ON45736–ON457959, KY587180, KY587181, MN984214, MN984217, HQ025929, and HQ025930; LaFond al. 2022) together, there were a total of 41 MHC alleles in the US and China, including 17 alleles in the US invaded range (6 privates), 29 alleles (17 privates) in the US native range, and 9 alleles (2 privates: RACA_03 and RACA_05) in Chinese populations. Figure 2B shows the phylogeny of these alleles, which were not clustered into invasive-only or native-only clades. One clade contained two alleles that were unique to invasive populations (ON457941 and ON457949), and one clade contained three alleles that were unique to native populations (ON477940, ON457947, and RACA_10).

We found no recombination of these alleles (STAR Methods). Four models (FEL [Fixed Effects Likelihood], FUBAR [A Fast, Unconstrained Bayesian AppRoximation for Inferring Selection], MEME [Detect Individual Sites Subject to Episodic Diversifying Selection], and SLAC [Single-Likelihood Ancestor Counting]) consistently detected two codons (codes 4 and 19) under positive selection (Table S5). Both codes 4 and 19 were in the PBS region. The aBSREL test indicated 4 branches (orange color, recent branches RACA_05 that was found in 5 populations in China: HS, ZB, LL, LS, and YZ [YZ=Yangzhou], and RACA_10 that was found in KS; the ancestral branch of ON457941 and ON457949, and the ancestral branch of ON457957 and RACA_02) leading to alleles under positive selection (Figure 2B).

According to the clusters of similar peptide-binding specificity, all MHC alleles clustered into six functional supertypes (Figures 2B and S4). These supertypes occurred in all US invasive and native ranges and Chinese invasive populations. Three alleles (ON457944, ON457937, and RACA_09) were grouped into supertype 1, which were close to each other (Figure 2B). Supertype 3 occurred in the upper part of the tree, while supertype 5 was distributed throughout the tree.

The average number of supertypes across all populations in the US and China was 2.56 $\pm$ 0.75 supertypes (Table S4), ranging from a minimum of 2 supertypes in most populations to 5 supertypes in KS (Table S4). There were no differences in each MHC diversity index (Na, Ho, He, number of supertypes, and π) among US native and invasive populations and Chinese invaded populations (Table S6, and Figures 3D–3H).

To determine if these patterns held in recent invasions, we reanalyzed the datasets excluding the Hansou population with the longest residence time of establishment in China. The results were similar (Table S7), with identical MHC variations and supertype numbers between Chinese invasive and US native populations but with differences in cytb diversity.

Genetic differentiations between US populations and Chinese populations

There were no differences in cytb and microsatellite F_{ST} between the Hansou population and CA or between CA and KS in the US (Tables S8 and S9). The average genetic differentiation coefficient (F_{ST}) was 0.23 $\pm$ 0.07 for MHC with 252/300 significant pairwise values in Chinese populations (Tables S8–S10), 0.22 $\pm$ 0.05 for cytb with 261/300, and 0.24 $\pm$ 0.08 for microsatellites with 257/300. No difference in average F_{ST} was detected among MHC, cytb, and microsatellites across Chinese populations (Table S10).

We compared the paired F_{ST} among the US native (9 populations excluding two populations without values) and invaded (8 populations excluding one population) ranges, and the Chinese invaded range (23 populations) (Table S10) and found no difference in MHC between the US native and Chinese invaded ranges,

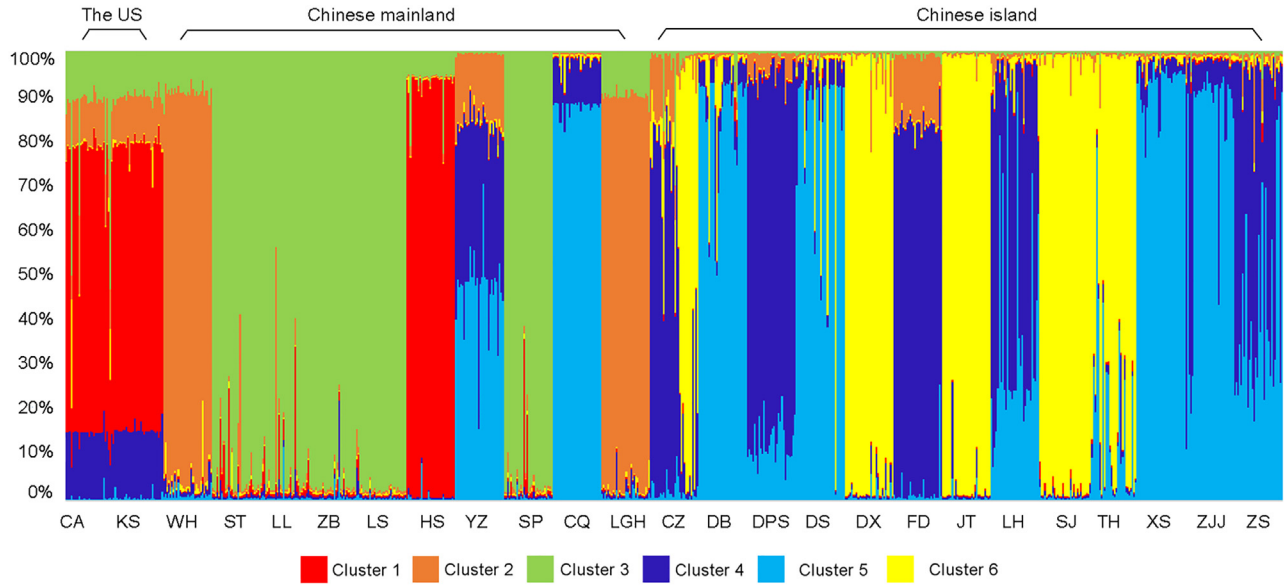

Figure 4. Population structure of 9 microsatellites generated from microsatellite STRUCTURE analysis based on allele frequency variation for all samples across 25 bullfrog populations in this study

Acronyms represent sample sites. Each individual is represented by a vertical line. Each color indicates a cluster.

but differences in MHC were detected between the US and Chinese invaded ranges, cytb between the Chinese invasive and US native populations, and between the Chinese and US invasive populations (Table S10).

Pathogen-mediated selection on Chinese bullfrog populations

Approximately 9.8% of samples (45/460 individuals) were Bd positive across 23 Chinese populations (19 populations infected), 40% of samples (8/20) in CA, and 55% (11/20) of samples in KS. Bd infection prevalence in 23 Chinese populations was lower than that in two US populations (CA and KS)[8] (Mann-Whitney U test, n = 25, $Z = 2.342$, p = 0.019). Furthermore, combined with data on Bd prevalence from LaFond et al. 2022, both US invasive (39.84% = 102/256 samples) (n = 34, $Z = 2.503$, p = 0.012) and native populations (26.70% = 59/221 samples) (n = 34, $Z = 2.787$, p = 0.005) had higher Bd prevalence than Chinese populations.

We recovered four Bd haplotypes from Chinese populations: CN18, CN15, CN25, and CN3. All of these haplotypes were previously identified in Chinese amphibians by Bai et al. (2014). Three of these haplotypes (CN18, CN15, and CN25) belonged to the BdGPL lineage (82.2% = 37/45 sequences), while CN3 belonged to the BdASIA lineage (17.8% = 8/45) (Figure S3). In two US populations (CA and KS), we identified two haplotypes, CN18 and CN28, both belonging to the BdGPL lineage.

Relative risk (RR) analysis of Bd infection for MHC alleles demonstrated that four alleles (RACA_01 = LiCa_B in LaFond et al. (2022), RACA_02, RACA_05, RACA_07 = Rapi_33) were associated with a significantly decreased risk of Bd infection (Fisher's exact test, $RR = 0.73$, p = 0.04 for RACA_01; $RR = 0.42$ p = 0.02 for RACA_02; $RR = 0.55$, p = 0.04 for RACA_05; $RR = 0.65$, p = 0.03 for RACA_07) (Figure 5), indicating that they were resistant to Bd infection. The RACA_06 (=LiCa_A) allele was associated with a significantly increased risk of Bd infection ($RR = 2.37$, p = 0.01), suggesting that this was susceptible to Bd infestation.

We also examined the relationships between MHC diversity or functional supertypes and the richness and abundance of pathogenic viruses in environments across 13 insular populations on the Zhoushan Archipelago, where data on environmental viruses were collected. We identified a total of 15 pathogenic virus species on the islands, including 14 DNA viruses (12 species of *Iridoviridae* and two of *Herpesviridae*) and one RNA virus in *Togaviridae* (Table S11). There were 6–13 viral species detected on an island. *FV3* was found to

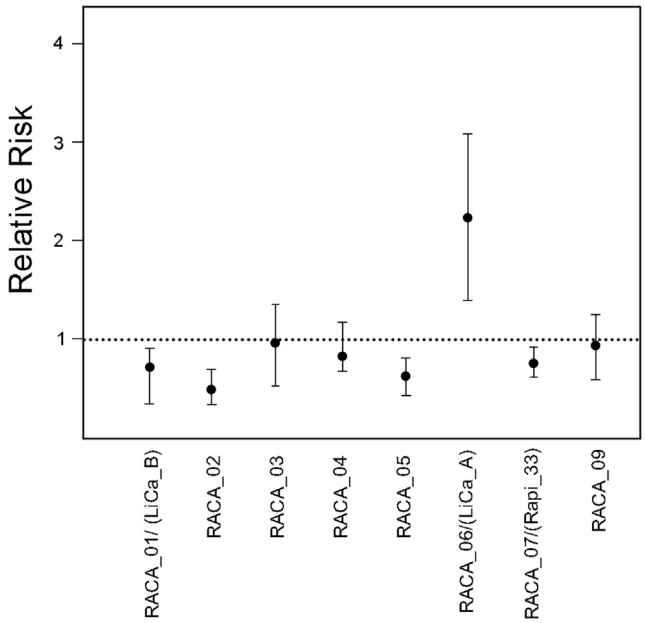

Figure 5. Relative risks of Bd infection among 10 MHC alleles across 23 Chinese bullfrog populations in this study
Error bars represent Wald confidence intervals. Values greater than one are associated with a significantly increased risk of Bd infection. Values less than one are associated with a significantly decreased risk of Bd infection.

have the highest abundance among viruses (23–243 sequences per sample), followed by *Ambystoma tigrinum* virus (3–62 sequences) and *invertebrate iridescent virus* 9 (3–56 sequences).

MHC allelic richness was positively correlated with both viral richness (Spearman rank correlation test, $R = 0.617$, $p = 0.03$) and viral abundance ($R = 0.844$ $p < 0.01$) (Figures 6A and 6B), but there was no correlation with number of microsatellites (Na) ($R = 0.369$, $p = 0.21$ for richness; $R = 0.305$, $p = 0.34$ for abundance) (Figures 6C and 6D), number of haplotypes of cytb gene ($R = 0.105$, $p = 0.93$ for richness; $R = 0.412$, $p = 0.16$ for abundance) (Figures 6E and 6F), and number of supertypes ($R = 0.025$, $p = 0.93$ for richness; $R = 0.39$, $p = 0.18$ for abundance) (Figures 6G and 6H). Furthermore, Na of MHC was positively correlated with the abundance of two specific viruses (FV3: $R = 0.812$, $p = 0.001$ for FV3; $R = 0.825$, $p < 0.001$ for *Ambystoma tigrinum* virus, significance level $\alpha = 0.00333$ (0.05/15) after Bonferroni correction) (Table S12).

DISCUSSION

We compared changes in genetic variations at neutral loci and an adaptive MHC gene in invasive bullfrog populations at large spatiotemporal scales. We found an approximately 60% reduction in the number of haplotypes, Hd and π at the neutral cytb gene across Chinese populations compared with those in US native populations and similar MHC diversity (Na, Ho, He, and π) and supertypes between Chinese invasive and US native populations. Some MHC alleles were associated with increased or decreased RR of Bd infection in Chinese populations. The MHC allele RACA_05, which is private to Chinese populations, was subjected to recent positive selection and was associated with a reduced risk of Bd infection. These results suggest that pathogen-mediated positive selection may promote adaptive MHC variations and functional diversity maintenance against serious founder effects in Chinese populations. As most Chinese populations have been established for less than 35 years or 15 generations at the sampling time, this study provides the first evidence that invasive populations can maintain both adaptive genetic variations and functional diversity in the very early stage of invasions.

Major studies on neutral loci (microsatellites, allozymes, mitochondrial genes, or nuclear sequences) show modest reductions in genetic variation in invasive populations (e.g., average loss of 15.5% and 18.7% of allelic diversity and heterozygosity, respectively) compared with source populations,[4] while some cases display higher levels of genetic diversity due to the admixture of multiple introductions from different

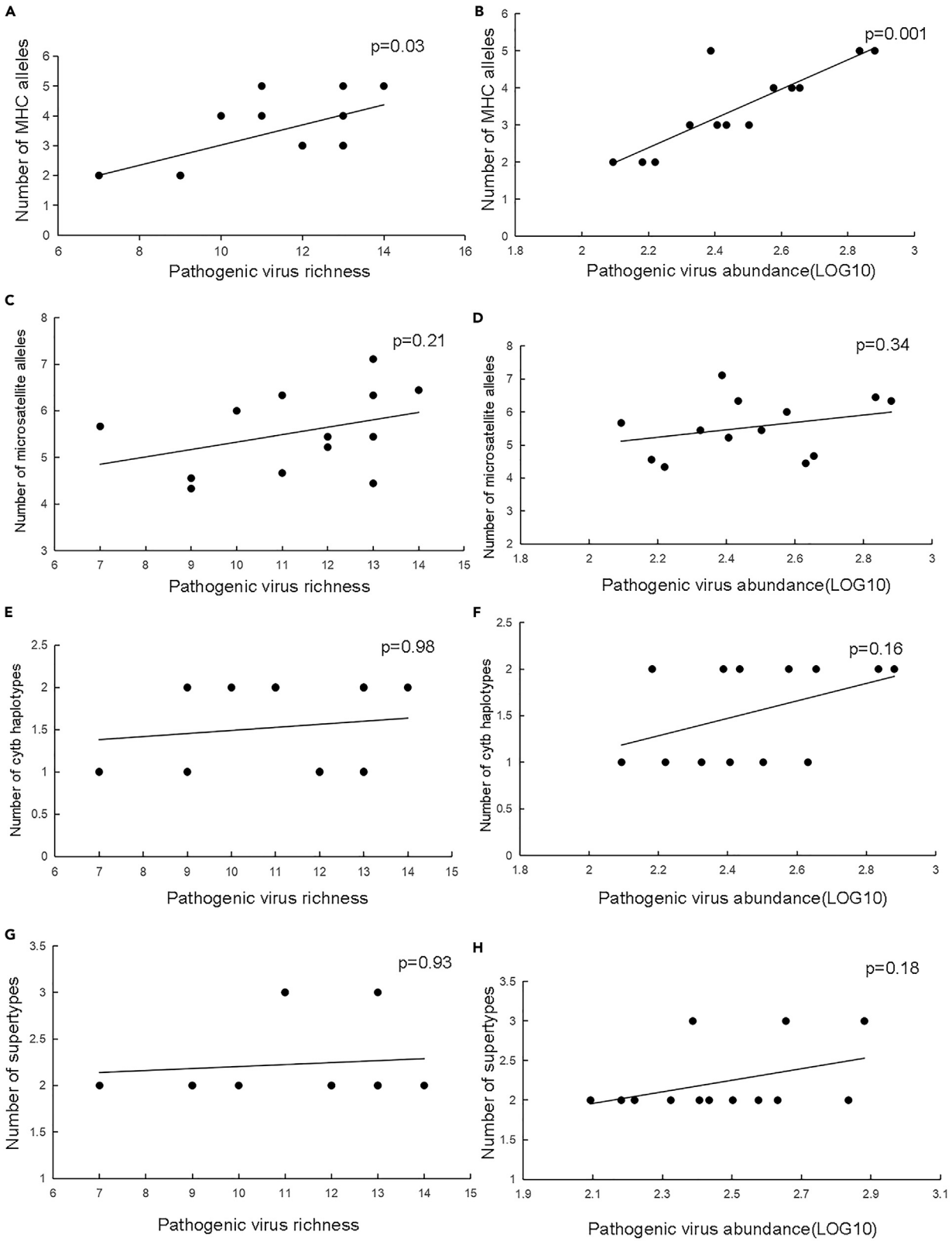
A
p=0.03
Number of MHC alleles
Pathogenic virus richness
B
p=0.001
Number of MHC alleles
Pathogenic virus abundance(LOG10)
C
p=0.21
Number of microsatellite alleles
Pathogenic virus richness
D
p=0.34
Number of microsatellite alleles
Pathogenic virus abundance(LOG10)
E
p=0.98
Number of cytb haplotypes
Pathogenic virus richness
F
p=0.16
Number of cytb haplotypes
Pathogenic virus abundance(LOG10)
G
p=0.93
Number of supertypes
Pathogenic virus richness
H
p=0.18
Number of supertypes
Pathogenic virus abundance(LOG10)

Figure 6. Spearman rank correlation tests on relationships between genetic diversity of cytb, microsatellites, or MHC and pathogenic virus richness and abundance on 13 islands of Zhoushan Archipelago, China

(A, C, E, and G) showed the spearman rank correlation tests on relationships between genetic diversity of cytb, microsatellites, or MHC and pathogenic virus richness.

(B, D, F, and H) showed the spearman rank correlation tests on relationships between genetic diversity of cytb, microsatellites, or MHC and pathogenic abundance (Spearman's p values are shown in the right corner of the plot).

source populations. Comparatively, Chinese bullfrog populations show serious population bottlenecks. Such bottlenecks may be because bullfrog farms in China generally use several pairs of adult frogs for a founder population.[22,23] Small founder populations and sequential founding events among bullfrog farms may contribute to a substantial reduction in neutral genetic diversity. The multiple clusters of microsatellites (Figure 4) indicate that Chinese populations might have been sourced from multiple introductions. Two haplotypes were shared with Hansou and CA (Figure 2B), and no difference in *Fst* for cytb and microsatellites was detected between Hansou and CA (Tables S7 and S8), suggesting CA as the most likely origin of the Hansou population. One plausible introduction pathway is that the Hansou population was introduced from the Cuba population, which was sourced from CA.[23] As many bullfrogs have been imported from China to California for years,[36] we could not exclude other explanations for lack of differences in *Fst* for cytb and microsatellites, that is, some bullfrog populations in California could be sourced from China.

No differences in adaptive MHC variations and functional diversity between Chinese invasive and US native populations mirrored recent work on adaptive MHC genes in animal invaders.[8,10] For example, Biedrzycka et al. (2020) compared genetic diversity at both neutral microsatellite loci and an MHC-DRB locus of native and invasive populations of raccoon (*Procyon lotor*), which was first introduced to Europe in the invaded range in the 1930s. They found that functional supertypes were maintained in the invasive region, while some MHC alleles were lost relative to native populations. LaFond et al. (2022) examined genetic diversity at the MHC class-II β gene and cytochrome *b* (cytb) loci for bullfrog populations across the invasive (established since at least 1904) and native ranges in North America and found that invasive populations had lower cytb diversity but maintained similar levels of MHC diversity. These studies, combined with our results, support the hypothesis that functional diversity maintenance at MHC genes may be a general pattern in invasive jawed vertebrates, which likely contributes to invasion success.

Pathogen-mediated balancing selection plays a role in driving MHC variations against serious founder effects in Chinese populations. Models predict that balancing selection can cause positive selection, maintain the polymorphism of MHC genes, and produce long genealogies.[11,37] Pathogenic Bd may affect MHC polymorphisms and the functional diversity of Chinese bullfrog populations. Bd is responsible for the decline of at least 500 amphibian species in Australia, Central America, South America, the Sierra Nevada in North America, and the Iberian Peninsula in Europe.[38,39] Native Asian amphibians generally show no clinical signs of chytridiomycosis and a low Bd prevalence,[28,40–43] with no declines in Asian amphibians reported.[38,44] The mass mortality of wild American bullfrogs at Finley Lake in the US was attributed to chytridiomycosis, and experimental evidence shows that bullfrogs were susceptible to Bd (one strain).[45] While Bataille[46] (2013) identified three Bd lineages (BdASIA, BdGPL, and BdBRAIL) infecting bullfrog populations in South Korea, we only detected BdGPL and BdASIA lineages infecting Chinese bullfrog populations, with BdGPL dominating the infection. Differences in the RR of Bd infection were detected among MHC alleles in Chinese bullfrog populations (Figure 5), indicating that Bd imposed selection pressure on MHC alleles. The private allele RACA_5 under recent positive selection was resistant to Bd infection, providing evidence for the link between the RR of Bd infection and positive selection in China. RACA_05 likely resulted from the mutation that occurred in MHC sequences that were phylogenetically close to RACA_09 (Figure 2B), and positive selection likely promoted the frequency of RACA_05. However, the Bd prevalence in Chinese bullfrog populations was low (9.8%) compared with that in native (26.7%) and invasive populations (39.84%) in the US. How such low Bd prevalence in Chinese bullfrog populations has imposed selection on the MHC gene and promoted its variations remain to be resolved. An alternative explanation is that some MHC alleles in China were beneficial to the founder effect (or holdover) of the source population in California where Bd was more prevalent, and exerted selection on bullfrog populations in the source environment. The lack of occurrence of RACA_05 (and RACA_03) in the US could be due to insufficient sampling in the US native and invasive range, which missed sampling this allele. Consistent with the work of LaFond et al. (2022), RACA_01 (=LiCA_B) and RACA_07 (=Rapi_33) or RACA_06 (=LiCa_A) showed decreased or increased RR of Bd infection in Chinese populations.

Positive effects of pathogenic virus richness and abundance on genetic variations in the MHC class-II β gene in Chinese bullfrog populations on the Zhoushan Archipelago are consistent with a study on the MHC class Ia locus in native frogs (*Pelophylax nigromaculatus*).[33] Evidence shows that local variation in pathogen species, abundance and/or virulence in environments affect MHC variations.[33,47] Spatial variations in the distribution of pathogens may drive local genetic adaptation, enhancing the rate of population divergence relative to neutral markers,[33,48–50] resulting in positive relationships between MHC polymorphisms and pathogenic virus richness or abundance on the islands. While this study only identified the correlations between variations in the MHC class-II β gene and environmental pathogenic viruses, more experimental evidence is needed to understand the effect of pathogenic viruses on this gene.

In conclusion, the results of this study provide no evidence supporting the genetic paradox of invasions at an adaptive MHC gene. Chinese invasive bullfrog populations maintained MHC genetic variations and functional diversity within less than 15 generations of invasions. Serious population bottlenecks due to the founder effect do not harm the adaptive immune potential of invasive bullfrogs in new pathogenic environments. Due to their immune adaptive potential, it would be difficult to control bullfrog populations if they spread. The best strategy for managing the risk of bullfrog invasions is to prevent escapes of bullfrogs from bullfrog farms or the releases of unwanted pets or for religious purposes. Once a bullfrog population is established, the efficient approach is to remove it as early as possible. Additionally, there is a need to understand how adaptive variations in other functional genes in invasive species respond to new environments.

Limitations of the study

The samples used in this study did not include bullfrog individuals from bullfrog farms or markets.

STAR★METHODS

Detailed methods are provided in the online version of this paper and include the following:

- KEY RESOURCES TABLE
- RESOURCE AVAILABILITY
  - Lead contact
  - Materials availability
  - Data and code availability
- EXPERIMENTAL MODEL AND SUBJECT DETAILS
  - Bullfrogs subjects
- METHOD DETAILS
  - Sampling for bullfrogs, Bd and pathogenic virus in environments
  - DNA extraction, sequencing and gene typing for bullfrogs
  - Bd DNA extraction and sequencing
  - Metagenomics of pathogenic viruses in environments on islands of the Zhoushan Archipelago
  - Statistical analysis
  - Statistical analysis
- ADDITIONAL RESOURCES

SUPPLEMENTAL INFORMATION

Supplemental information can be found online at https://doi.org/10.1016/j.isci.2023.107316.

ACKNOWLEDGMENTS

We thank for Dr. Xuan Liu helping for bullfrog sample collection from America, and for Fort Hays State University's Sternberg Museum, and Museum of Vertebrate Zoology, University of California at Berkeley, for donating the bullfrog samples. We are grateful to two anonymous reviewers for their helpful comments, which improve the manuscript. This study is supported by grants from National Science Foundation of China (32030070), Second Tibetan Plateau Scientific Expedition and Research (STEP) Program (2019QZKK0501), the High-Level Talents Research Start-Up Project of Hebei University (050001–521100222045), Hebei Natural Science Foundation (C2022201042), and China's Biodiversity Observation Network (Sino-BON).

AUTHOR CONTRIBUTIONS

Y.L. and J.Z. designed the study; S.W. and Y.L. collected samples; J.Z., S.W., C.X., J.D., M.N., and J.Y. performed experiments; J.Z. and Y.L. analyzed the data; J.Z. and L.Y. wrote manuscript.

DECLARATION OF INTERESTS

The authors have no financial conflicts of interest.

INCLUSION AND DIVERSITY

We support inclusive, diverse, and equitable conduct of research.

Received: April 8, 2023
Revised: May 22, 2023
Accepted: July 4, 2023
Published: July 10, 2023

REFERENCES

1. Wang, S., Deng, T., Zhang, J., and Li, Y. (2023). Global economic costs of mammal invasions. Sci. Total Environ. *857*, 159479.

2. Diagne, C., Leroy, B., Gozlan, R.E., Vaissière, A.C., Assailly, C., Nuninger, L., Roiz, D., Jourdain, F., Jarić, I., and Courchamp, F. (2020). InvaCost, a public database of the economic costs of biological invasions worldwide. Sci. Data *7*, 277.

3. Blackburn, T.M., Bellard, C., and Ricciardi, A. (2019). Alien versus native species as drivers of recent extinctions. Front. Ecol. Environ. *17*, 203–207.

4. Estoup, A., Ravigné, V., Hufbauer, R., Vitalis, R., Gautier, M., and Facon, B. (2016). Is there a genetic paradox of biological invasion? Annu. Rev. Ecol. Evol. Syst. *47*, 51–72.

5. Dlugosch, K.M., and Parker, I.M. (2008). Invading populations of an ornamental shrub show rapid life history evolution despite genetic bottlenecks. Ecol. Lett. *11*, 701–709. https://doi.org/10.1111/j.1461-0248.2008.01181.x.

6. Teixeira, J.C., and Huber, C.D. (2021). The inflated significance of neutral genetic diversity in conservation genetics. Proc. Natl. Acad. Sci. USA *118*, e2015096118.

7. Hoelzel, A.R., Bruford, M.W., and Fleischer, R.C. (2019). Conservation of Adaptive Potential and Functional Diversity (Springer).

8. LaFond, J., Martin, K.R., Dahn, H., Richmond, J.Q., Murphy, R.W., Rollinson, N., and Savage, A.E. (2022). Invasive Bullfrogs Maintain MHC Polymorphism Including Alleles Associated with Chytrid Fungal Infection. Integr. Comp. Biol. *62*, 262–274. https://doi.org/10.1093/icb/icac044.

9. Wellband, K.W., Pettitt-Wade, H., Fisk, A.T., and Heath, D.D. (2018). Standing genetic diversity and selection at functional gene loci are associated with differential invasion success in two non-native fish species. Mol. Ecol. *27*, 1572–1585. https://doi.org/10.1111/mec.14557.

10. Biedrzycka, A., Konopiński, M., Hoffman, E., Trujillo, A., and Zalewski, A. (2020). Comparing raccoon major histocompatibility complex diversity in native and introduced ranges: Evidence for the importance of functional immune diversity for adaptation and survival in novel environments. Evol. Appl. *13*, 752–767. https://doi.org/10.1111/eva.12898.

11. Radwan, J., Babik, W., Kaufman, J., Lenz, T.L., and Winternitz, J. (2020). Advances in the Evolutionary Understanding of MHC Polymorphism. Trends Genet. *36*, 298–311. https://doi.org/10.1016/j.tig.2020.01.008.

12. Kaufman, J. (2018). Generalists and specialists: a new view of how MHC class I molecules fight infectious pathogens. Trends Immunol. *39*, 367–379.

13. Hughes, A.L., and Yeager, M. (1998). Natural selection and the evolutionary history of major histocompatibility complex loci. Front. Biosci. *3*, 509–516.

14. Milinski, M. (2006). The Major Histocompatibility Complex, Sexual Selection, and Mate Choice. Annu. Rev. Ecol. Evol. Syst. *37*, 159–186. https://doi.org/10.1146/annurev.ecolsys.37.091305.110242.

15. Spurgin, L.G., and Richardson, D.S. (2010). How pathogens drive genetic diversity: MHC, mechanisms and misunderstandings. Proc. Biol. Sci. *277*, 979–988. https://doi.org/10.1098/rspb.2009.2084.

16. Doytchinova, I.A., and Flower, D.R. (2005). In silico identification of supertypes for class II MHCs. J. Immunol. *174*, 7085–7095. https://doi.org/10.4049/jimmunol.174.11.7085.

17. Wang, M., and Claesson, M.H. (2014). Classification of Human Leukocyte Antigen (HLA) Supertypes (Immunoinformatics), pp. 309–317.

18. Lowe, S., Browne, M., Boudjelas, S., and De Poorter, M. (2000). 100 of the World's Worst Invasive Alien Species: A Selection from the Global Invasive Species Database (Invasive Species Specialist Group Auckland).

19. Bury, R.B., and Whelan, J.A. (1984). Ecology and Management of the Bullfrog (US Department of the Interior, Fish and Wildlife Service).

20. Kats, L.B., and Ferrer, R.P. (2003). Alien predators and amphibian declines: review of two decades of science and the transition to conservation. Divers. Distrib. *9*, 99–110.

21. Ficetola, G.F., Thuiller, W., and Miaud, C. (2007). Prediction and validation of the potential global distribution of a problematic alien invasive species — the American bullfrog. Divers. Distrib. *13*, 476–485. https://doi.org/10.1111/j.1472-4642.2007.00377.x.

22. Li, Y., Ke, Z., Wang, Y., and Tim, B. (2011). Frog Community Responses to Recent American Bullfrog Invasions.

23. Bai, C., Ke, Z., Consuegra, S., Liu, X., and Li, Y. (2012). The role of founder effects on the genetic structure of the invasive bullfrog (Lithobates catesbeianaus) in China. Biol. Invasions *14*, 1785–1796. https://doi.org/10.1007/s10530-012-0189-x.

24. Liu, X., and Li, Y. (2009). Aquaculture enclosures relate to the establishment of feral populations of introduced species. PLoS One *4*, e6199. https://doi.org/10.1371/journal.pone.0006199.

25. Liu, X., McGarrity, M.E., Bai, C., Ke, Z., and Li, Y. (2013). Ecological knowledge reduces religious release of invasive species. Ecosphere *4*, art21. https://doi.org/10.1890/es12-00368.1.

26. Wang, S., Liu, C., Wu, J., Xu, C., Zhang, J., Bai, C., Gao, X., Liu, X., Li, X., Zhu, W., and Li, Y. (2019). Propagule pressure and hunting pressure jointly determine genetic evolution in insular populations of a global frog invader. Sci. Rep. *9*, 448. https://doi.org/10.1038/s41598-018-37007-6.

27. Garner, T.W.J., Perkins, M.W., Govindarajulu, P., Seglie, D., Walker, S., Cunningham, A.A., and Fisher, M.C. (2006). The emerging amphibian pathogen Batrachochytrium dendrobatidis globally infects introduced

populations of the North American bullfrog, Rana catesbeiana. Biol. Lett. *2*, 455–459.

28. Bai, C., Liu, X., Fisher, M.C., Garner, T.W.J., and Li, Y. (2012). Global and endemic Asian lineages of the emerging pathogenic fungus Batrachochytrium dendrobatidis widely infect amphibians in China. Divers. Distrib. *18*, 307–318. https://doi.org/10.1111/j.1472-4642.2011.00878.x.

29. Brunner, J.L., Olson, A.D., Rice, J.G., Meiners, S.E., Le Sage, M.J., Cundiff, J.A., Goldberg, C.S., and Pessier, A.P. (2019). Ranavirus infection dynamics and shedding in American bullfrogs: Consequences for spread and detection in trade. Dis. Aquat. Org. *135*, 135–150.

30. Miller, D.L., Rajeev, S., Gray, M.J., and Baldwin, C.A. (2007). Frog virus 3 infection, cultured American bullfrogs. Emerg. Infect. Dis. *13*, 342–343.

31. Savage, A.E., and Zamudio, K.R. (2011). MHC genotypes associate with resistance to a frog-killing fungus. Proc. Natl. Acad. Sci. USA *108*, 16705–16710.

32. Savage, A.E., and Zamudio, K.R. (2016). Adaptive tolerance to a pathogenic fungus drives major histocompatibility complex evolution in natural amphibian populations. Proc. Biol. Sci. *283*, 20153115.

33. Wang, S., Liu, C., Wilson, A.B., Zhao, N., Li, X., Zhu, W., Gao, X., Liu, X., and Li, Y. (2017). Pathogen richness and abundance predict patterns of adaptive major histocompatibility complex variation in insular amphibians. Mol. Ecol. *26*, 4671–4685.

34. Mulder, K.P., Cortazar-Chinarro, M., Harris, D.J., Crottini, A., Campbell Grant, E.H., Fleischer, R.C., and Savage, A.E. (2017). Evolutionary dynamics of an expressed MHC class IIbeta locus in the Ranidae (Anura) uncovered by genome walking and high-throughput amplicon sequencing. Dev. Comp. Immunol. *76*, 177–188. https://doi.org/10.1016/j.dci.2017.05.022.

35. Trujillo, A.L., Hoffman, E.A., Becker, C.G., and Savage, A.E. (2021). Spatiotemporal adaptive evolution of an MHC immune gene in a frog-fungus disease system. Heredity *126*, 640–655.

36. Schloegel, L.M., Picco, A.M., Kilpatrick, A.M., Davies, A.J., Hyatt, A.D., and Daszak, P. (2009). Magnitude of the US trade in amphibians and presence of Batrachochytrium dendrobatidis and ranavirus infection in imported North American bullfrogs (Rana catesbeiana). Biol. Conserv. *142*, 1420–1426.

37. Takahata, N., and Nei, M. (1990). Allelic genealogy under overdominant and frequency-dependent selection and polymorphism of major histocompatibility complex loci. Genetics *124*, 967–978.

38. Scheele, B.C., Pasmans, F., Skerratt, L.F., Berger, L., Martel, A., Beukema, W., Acevedo, A.A., Burrowes, P.A., Carvalho, T., Catenazzi, A., et al. (2019). Amphibian fungal panzootic causes catastrophic and ongoing loss of biodiversity. Science *363*, 1459–1463.

39. O'hanlon, S.J., Rieux, A., Farrer, R.A., Rosa, G.M., Waldman, B., Bataille, A., Kosch, T.A., Murray, K.A., Brankovics, B., Fumagalli, M., et al. (2018). Recent Asian origin of chytrid fungi causing global amphibian declines. Science *360*, 621–627.

40. Goka, K., Yokoyama, J., Une, Y., Kuroki, T., Suzuki, K., Nakahara, M., Kobayashi, A., Inaba, S., Mizutani, T., and Hyatt, A.D. (2009). Amphibian chytridiomycosis in Japan: distribution, haplotypes and possible route of entry into Japan. Mol. Ecol. *18*, 4757–4774. https://doi.org/10.1111/j.1365-294X.2009.04384.x.

41. Zhu, W., Fan, L., Soto-Azat, C., Yan, S., Gao, X., Liu, X., Wang, S., Liu, C., Yang, X., and Li, Y. (2016). Filling a gap in the distribution of Batrachochytrium dendrobatidis: evidence in amphibians from northern China. Dis. Aquat. Org. *118*, 259–265. https://doi.org/10.3354/dao02975.

42. Swei, A., Jodi, J., Rowley, L., Rödder, D., Mae, L., Diesmos, L., Diesmos, A.C., Briggs, C.J., Brown, R., Cao, T.T., Cheng, T.L., Chong, R.A., et al. (2011). Is Chytridiomycosis an Emerging Infectious Disease in Asia? PLoS One *8*. https://doi.org/10.1371/journal.pone.0023179.

43. Dahanukar, N., Krutha, K., Paingankar, M.S., Padhye, A.D., Modak, N., and Molur, S. (2013). Endemic Asian chytrid strain infection in threatened and endemic anurans of the Northern Western Ghats, India. PLoS One *8*, e77528. https://doi.org/10.1371/journal.pone.0077528.

44. Fu, M., and Waldman, B. (2019). Ancestral chytrid pathogen remains hypervirulent following its long coevolution with amphibian hosts. Proc. Biol. Sci. *286*, 20190833. https://doi.org/10.1098/rspb.2019.0833.

45. Gervasi, S.S., Urbina, J., Hua, J., Chestnut, T., A Relyea, R., and R Blaustein, A. (2013). Experimental evidence for American bullfrog (Lithobates catesbeianus) susceptibility to chytrid fungus (Batrachochytrium dendrobatidis). EcoHealth *10*, 166–171.

46. Bataille, A., Fong, J.J., Cha, M., Wogan, G.O.U., Baek, H.J., Lee, H., Min, M.-S., and Waldman, B. (2013). Genetic evidence for a high diversity and wide distribution of endemic strains of the pathogenic chytrid fungus Batrachochytrium dendrobatidis in wild Asian amphibians. Mol. Ecol. *22*, 4196–4209. https://doi.org/10.1111/mec.12385.

47. Eizaguirre, C., Lenz, T.L., Kalbe, M., and Milinski, M. (2012). Rapid and adaptive evolution of MHC genes under parasite selection in experimental vertebrate populations. Nat. Commun. *3*, 621. https://doi.org/10.1038/ncomms1632.

48. Loiseau, C., Richard, M., Garnier, S., Chastel, O., Julliard, R., Zoorob, R., and Sorci, G. (2009). Diversifying selection on MHC class I in the house sparrow (Passer domesticus). Mol. Ecol. *18*, 1331–1340.

49. Marsden, C.D., Woodroffe, R., Mills, M.G.L., McNUTT, J.W., Creel, S., Groom, R., Emmanuel, M., Cleaveland, S., Kat, P., Rasmussen, G.S.A., et al. (2012). Spatial and temporal patterns of neutral and adaptive genetic variation in the endangered African wild dog (Lycaon pictus). Mol. Ecol. *21*, 1379–1393.

50. Savage, A.E., and Zamudio, K.R. (2016). Adaptive tolerance to a pathogenic fungus drives major histocompatibility complex evolution in natural amphibian populations. Proc. Biol. Sci. *283*, 20153115. https://doi.org/10.1098/rspb.2015.3115.

51. Thurber, R.V., Haynes, M., Breitbart, M., Wegley, L., and Rohwer, F. (2009). Laboratory procedures to generate viral metagenomes. Nat. Protoc. *4*, 470–483. https://doi.org/10.1038/nprot.2009.10.

52. Ewels, P., Magnusson, M., Lundin, S., and Käller, M. (2016). MultiQC: summarize analysis results for multiple tools and samples in a single report. Bioinformatics *32*, 3047–3048.

53. Zhang, J., Kobert, K., Flouri, T., and Stamatakis, A. (2014). PEAR: a fast and accurate Illumina Paired-End reAd mergeR. Bioinformatics *30*, 614–620.

54. Sommer, S., Courtiol, A., and Mazzoni, C.J. (2013). MHC genotyping of non-model organisms using next-generation sequencing: a new methodology to deal with artefacts and allelic dropout. BMC Genom. *14*, 542–617.

55. Sebastian, A., Herdegen, M., Migalska, M., and Radwan, J. (2016). AMPLISAS: a web server for multilocus genotyping using next-generation amplicon sequencing data. Mol. Ecol. Resour. *16*, 498–510. https://doi.org/10.1111/1755-0998.12453.

56. Austin, J.D., Dávila, J.A., Lougheed, S.C., and Boag, P.T. (2003). Genetic evidence for female-biased dispersal in the bullfrog, Rana catesbeiana (Ranidae). Mol. Ecol. *12*, 3165–3172. https://doi.org/10.1046/j.1365-294x.2003.01948.x.

57. Van Oosterhout, C., Hutchinson, W.F., Wills, D.P.M., and Shipley, P. (2004). micro-checker: software for identifying and correcting genotyping errors in microsatellite data. Mol. Ecol. Notes *4*, 535–538. https://doi.org/10.1111/j.1471-8286.2004.00684.x.

58. Raymond, M., and Rousset, F. (1995). Population Genetics Software for Exact Tests and Ecumenicism. J. Hered. *86*, 248–249.

59. Annis, S.L., Dastoor, F.P., Ziel, H., Daszak, P., and Longcore, J.E. (2004). A DNA-based assay identifies Batrachochytrium dendrobatidis in amphibians. J. Wildl. Dis. *40*, 420–428.

60. Ge, X., Li, Y., Yang, X., Zhang, H., Zhou, P., Zhang, Y., and Shi, Z. (2012). Metagenomic analysis of viruses from bat fecal samples reveals many novel viruses in insectivorous bats in China. J. Virol. *86*, 4620–4630.

61. Densmore, C.L., and Green, D.E. (2007). Diseases of amphibians. ILAR J. *48*, 235–254.

62. Duffus, A.L., Waltzek, T.B., Stöhr, A.C., Allender, M.C., Gotesman, M., Whittington, R.J., Hick, P., Hines, M.K., and Marschang,

R.E. (2015). Distribution and host range of ranaviruses. Ranaviruses: Lethal pathogens of ectothermic vertebrates, 9–57.

63. Peakall, R.O.D., and Smouse, P.E. (2006). genalex 6: genetic analysis in Excel. Population genetic software for teaching and research. Mol. Ecol. Notes *6*, 288–295. https://doi.org/10.1111/j.1471-8286.2005.01155.x.

64. Pritchard, J.K., Stephens, M., and Donnelly, P. (2000). Inference of Population Structure Using Multilocus Genotype Data. Genetics *155*, 945–959.

65. Evanno, G., Regnaut, S., and Goudet, J. (2005). Detecting the number of clusters of individuals using the software STRUCTURE: a simulation study. Mol. Ecol. *14*, 2611–2620. https://doi.org/10.1111/j.1365-294X.2005.02553.x.

66. Earl, D.A., and vonHoldt, B.M. (2011). STRUCTURE HARVESTER: a website and program for visualizing STRUCTURE output and implementing the Evanno method. Conserv. Genet. Resour. *4*, 359–361. https://doi.org/10.1007/s12686-011-9548-7.

67. Sommer, S., Courtiol, A., and Mazzoni, C.J. (2013). MHC Genotyping of Non-model Organisms Using Next-Generation Sequencing: A New Methodology to Deal with Artefacts and Allelic Dropout.

68. Rousset, F., Lopez, J., and Belkhir, K. (2020). Package 'genepop'.

69. Goudet, J. (2002). FSTAT, a program to estimate and test gene diversities and fixation indices. Version 2.9. 3.2. http://www.unil.ch/izea/softwares/fstat.html.

70. Excoffier, L., Laval, G., and Schneider, S. (2007). Arlequin (version 3.0): an integrated software package for population genetics data analysis. Evol. Bioinform. Online *1*, 47–50.

71. Leigh, J.W., and Bryant, D. (2015). POPART: full-feature software for haplotype network construction. Methods Ecol. Evol. *6*, 1110–1116.

72. Kumar, S., Stecher, G., and Tamura, K. (2016). MEGA7: Molecular Evolutionary Genetics Analysis Version 7.0 for Bigger Datasets. Mol. Biol. Evol. *33*, 1870–1874. https://doi.org/10.1093/molbev/msw054.

73. Lanfear, R., Frandsen, P.B., Wright, A.M., Senfeld, T., and Calcott, B. (2017). PartitionFinder 2: new methods for selecting partitioned models of evolution for molecular and morphological phylogenetic analyses. Mol. Biol. Evol. *34*, 772–773.

74. Ronquist, F., Teslenko, M., Van Der Mark, P., Ayres, D.L., Darling, A., Höhna, S., Larget, B., Liu, L., Suchard, M.A., and Huelsenbeck, J.P. (2012). MrBayes 3.2: efficient Bayesian phylogenetic inference and model choice across a large model space. Syst. Biol. *61*, 539–542.

75. Rambaut, A., Drummond, A.J., Xie, D., Baele, G., and Suchard, M.A. (2018). Posterior summarization in Bayesian phylogenetics using Tracer 1.7. Syst. Biol. *67*, 901–904.

76. Martin, D.P., Lemey, P., Lott, M., Moulton, V., Posada, D., and Lefeuvre, P. (2010). RDP3: a flexible and fast computer program for analyzing recombination. Bioinformatics *26*, 2462–2463.

77. Kosakovsky Pond, S.L., and Frost, S.D.W. (2005). Not so different after all: a comparison of methods for detecting amino acid sites under selection. Mol. Biol. Evol. *22*, 1208–1222.

78. Murrell, B., Wertheim, J.O., Moola, S., Weighill, T., Scheffler, K., and Kosakovsky Pond, S.L. (2012). Detecting individual sites subject to episodic diversifying selection. PLoS Genet. *8*, e1002764. https://doi.org/10.1371/journal.pgen.1002764.

79. Brown, J.H., Jardetzky, T.S., Gorga, J.C., Stern, L.J., Urban, R.G., Strominger, J.L., and Wiley, D.C. (1993). Three-dimensional structure of the human class II histocompatibility antigen HLA-DR1. Nature *364*, 33–39.

80. Tong, J.C., Bramson, J., Kanduc, D., Chow, S., Sinha, A.A., and Ranganathan, S. (2006). Modeling the bound conformation of Pemphigus vulgaris-associated peptides to MHC Class II DR and DQ alleles. Immunome Res. *2*, 1. https://doi.org/10.1186/1745-7580-2-1.

81. Jombart, T., Devillard, S., and Balloux, F. (2010). Discriminant analysis of principal components: a new method for the analysis of genetically structured populations. BMC Genet. *11*, 94.

82. Jombart, T., and Ahmed, I. (2011). adegenet 1.3-1: new tools for the analysis of genome-wide SNP data. Bioinformatics *27*, 3070–3071.

83. Sergeant, E., Nunes, T., Marshall, J., Sanchez, J., Thorn-Ton, R., Reiczigel, J., Robison-Cox, J., Sebastiani, P., Solymos, P., and Yoshida, K. (2021). Package "epiR" Title Tools for the Analysis of Epidemiological Data.

84. Tamura, K., Peterson, D., Peterson, N., Stecher, G., Nei, M., and Kumar, S. (2011). MEGA5: molecular evolutionary genetics analysis using maximum likelihood, evolutionary distance, and maximum parsimony methods. Mol. Biol. Evol. *28*, 2731–2739. https://doi.org/10.1093/molbev/msr121.

85. Nei, M., and Kumar, S. (2000). Molecular Evolution and Phylogenetics (Oxford University Press).

86. Stamatakis, A. (2006). RAxML-VI-HPC: maximum likelihood-based phylogenetic analyses with thousands of taxa and mixed models. Bioinformatics *22*, 2688–2690.

87. Stamatakis, A., Hoover, P., and Rougemont, J. (2008). A rapid bootstrap algorithm for the RAxML web servers. Syst. Biol. *57*, 758–771.

88. Ronquist, F., and Huelsenbeck, J.P. (2003). MrBayes 3: Bayesian phylogenetic inference under mixed models. Bioinformatics *19*, 1572–1574.

89. Posada, D. (2008). jModelTest: phylogenetic model averaging. Mol. Biol. Evol. *25*, 1253–1256.

90. Wilgenbusch, J.C., Warren, D.L., and Swofford, D.L. (2004). AWTY: A system for graphical exploration of MCMC convergence in Bayesian phylogenetic inference[J].

91. Bandelt, H.-J., Forster, P., and Röhl, A. (1999). Median-joining networks for inferring intraspecific phylogenies. Mol. Biol. Evol. *16*, 37–48.

STAR★METHODS

KEY RESOURCES TABLE

REAGENT or RESOURCE	SOURCE	IDENTIFIER
Bacterial and virus strains		
Pathogenic virus	sampled in our previous study	see Table S11
Biological samples		
Bullfrog samples	sampled in this study	see Table S1
Chemicals, peptides, and recombinant proteins		
DNA polymerase	TransGen	TransStart® FastPfu DNA Polymerase
RNA Kit	Qiagen	QIAamp Viral RNA Kit
Deposited data		
MHC sequences	Obtained from GenBank	ON457936-ON457959 , HQ025929-HQ025931, KY587180-KY587181 , MN984214 , MN984217
Cytb haplotypes	Obtained from GenBank	ON457960-ON457993
Software and algorithms		
R Version4.2.2	R Core Team	https://www.r-project.org/index.html
Fastqc v0.12.1	Simon Andrews	https://www.bioinformatics.babraham.ac.uk/projects/fastqc/
PEAR v0.9.8	Alexandros Stamatakis	https://cme.h-its.org/exelixis/web/software/pear/
AmpliSAS	Alvaro Sebastian	http://evobiolab.biol.amu.edu.pl/amplisat/index.php?amplisas
MICRO-CHECKER 2.2.3	Cock van Oosterhout	https://mybiosoftware.com/micro-checker-2-2-3-microsatellite-data-checking-software.html
GENEPOP v4.7.5	Raymond	https://genepop.curtin.edu.au/
GenAlEx v6.5	Peakall, R. and Smouse P.E.	https://biology-assets.anu.edu.au/GenAlEx/Welcome.html
STRUCTURE v2.3.4	Pritchard Lab	https://web.stanford.edu/group/pritchardlab/structure_software/release_versions/v2.3.4/html/structure.html
STRUCTURE HARVESTER	Earl, Dent A. and vonHoldt, Bridgett M.	https://taylor0.biology.ucla.edu/structureHarvester/
DnaSP6	Julio Rozas	http://www.ub.edu/dnasp/downloadTv6.html
FSTAT v2.9.4	Jérôme Goudet	https://www2.unil.ch/popgen/softwares/fstat.htm
Arlequin 3.11	Excoffier, L. G. Laval, and S. Schneider	http://cmpg.unibe.ch/software/arlequin3/
POPART v1.7	University of Otago Popart	https://popart.maths.otago.ac.nz/
MEGA7	Molecular Biology and Evolution	https://www.megasoftware.net/
PartitionFinder v2.1.1	Molecular Evolution and Phylogenetics	https://www.robertlanfear.com/partitionfinder/
Tracer v1.7	Molecular Evolution, Phylogenetics and Epidemiology	http://tree.bio.ed.ac.uk/software/tracer/
RDP 3.44	Darren Martin	https://www.softpedia.com/get/Science-CAD/RDP.shtml
Datamonkey server	Sergei L Kosakovsky Pond	https://www.datamonkey.org/

RESOURCE AVAILABILITY

Lead contact

Further information and requests for resources and reagents should be directed to and will be fulfilled by the lead contact, Yiming Li (liym@ioz.ac.cn).

Materials availability

All the requests for the bullfrog samples and data should be directed to the lead contact and will be made available on request after completion of a Materials Transfer Agreement.

Data and code availability

- MHC data is publicly available as of the date after publication. Accession numbers are listed in the additional resources.
- All original code and any additional information required to reanalyze the data reported in this paper are available from the lead contact upon reasonable request.
- All data generated during this study are available from the lead contact upon reasonable request.

EXPERIMENTAL MODEL AND SUBJECT DETAILS

Bullfrogs subjects

A total of 500 bullfrog toe samples were used in the experiment, including 460 samples collected in China and 40 samples donated by Fort Hays State University's Sternberg Museum and Museum of Vertebrate Zoology, University of California at Berkeley. All bullfrog toe samples were collected from mature bullfrog individuals, and both male and female bullfrogs were sampled in this study. No mouse experienced any manipulation other than standard husbandry and those described here. The methods were designed based on the Good Experimental Practices adopted by the Institute of Zoology, Chinese Academy of Sciences, China. All experimental procedures and animal collection were approved by the Animal Ethics Committee at the Institute of Zoology, Chinese Academy of Sciences, China (Permit Number: IOZ10013). All methods were carried out in accordance with relevant guidelines and regulations.

METHOD DETAILS

Sampling for bullfrogs, Bd and pathogenic virus in environments

We collected 20 postmetamorphic individuals of 23 feral bullfrog populations across 9 provinces in China between May and October from 2010-2017 (Table S1), including 9 mainland populations, 13 insular populations on 13 islands of the Zhoushan Archipelago, Zhejiang Province, and one insular population in Guangdong Province. We also obtained samples of bullfrogs from Fort Hays State University's Sternberg Museum and the Museum of Vertebrate Zoology, University of California at Berkeley, United States. To prevent the transfer of infected materials among sites and animals, we cleared boots and equipment with 5% bleach before sampling at a site. We captured bullfrogs in invaded waterbodies manually or with long-handled nets. We handled a frog with nonpowdered latex gloves and clipped the top one-third of the third toe of the right hind foot. The gloves were used only once for each frog and were discarded after sampling. The sampled frog was released at its capture site. We preserved each toe tip in a centrifuge tube with 95% ethanol and stored it at −20°C in a refrigerator.

We also collected data on the date of the first introduction of bullfrog populations across each invaded site based on questionnaire surveys of bullfrog farmers or residents around invaded sites.[24,26] The introduced date was defined as the year since the farm began to raise bullfrogs. If such information was not available at a site, we used the introduced date exactly as found in the reference.

We sampled soil and water for environmental pathogenic viruses at bullfrog collection sites on 13 islands of the Zhoushan Archipelago between May and July 2017.[33] On each island, we collected five water samples (1 L per sample) from surface water along the shores of invaded waterbodies (ponds, reservoirs, rice fields) at random and combined them for analysis. We also collected five samples of 500 g surface soil onshores using a clean trowel. We homogenized and sorted soil samples through a 2-mm sieve and maintained the samples at 4°C until analysis. In the laboratory, we made soil supernatant for each sample following Wang et al. (2017). We combined 1 L of soil supernatant and 1 L of water samples from each site and concentrated them through filters (0.45 lm).[51] We collected 40 ml of concentrated filtrate stored at 4°C for metagenomics analysis.

DNA extraction, sequencing and gene typing for bullfrogs

DNA extraction We extracted bullfrog DNA following the procedure by Wang et al. (2019). We clipped a toe tip sample (approximately 3 mg) in a 2-ml centrifuge tube with 100 μl of lysis buffer containing 0.01 M NaCl, 0.1 M EDTA, 1 mg/ml proteinase K, 0.01 M Tris–HCl (pH 8.0) and 0.5% Nonidet P-40. The tube was vortexed for 1 min at ambient temperature, centrifuged to recover all materials from the bottom of the tube, and incubated at 50°C for 120 min and at 95°C for 20 min. The tube was centrifuged at 12,000 rpm

for 3 min at a cold temperature, and the extract was diluted to one tenth of its original concentration to amplify the DNA by polymerase chain reaction (PCR).

Amplification of MHC class-II β gene Following the procedure developed by Mulder et al. (2017),[34] the MHC class-II β gene was amplified using 20 pairs of the primers ForN and RevA attached with an 8 bp barcode, to distinguish different individuals in each population. PCRs were run with Pfu DNA polymerase (TransGen, Beijing, China) with several steps, including a denaturing step at 95°C for 2 min, followed by 35 cycles of 95°C for 20 s, 51°C for 20 s, and 72°C for 30 s, and a final extension of 5 min at 72°C. To assess possible PCR and sequencing artifacts, we amplified an additional six samples by random selection twice based on different fusion primer pairs and sequenced them across independent runs. We did not find sequencing artifacts for each PCR run. The amplification products were sequenced on an Illumina HiSeq2500 platform (Novogene Bioinformatics Technology Company, Beijing, China) using a 250-bp paired-end strategy, and all samples were run in a single lane.

We used Fastqc/Multiqc[52] to visualize MHC read quality, determined trimming parameters, and joined demultiplexed, paired-end reads with PEAR v0.9.8[53] using default parameters and a PHRED score cutoff of 20. AmpliSAS was used to cluster, filter and genotype the obtained sequences to discard sequences of the wrong length, sequences that did not blast to MHC, or sequences that had stop codons and only retained alleles that were recovered from at least 2 different individuals.[54] Following recommendations of clustering parameters for Illumina data[35,55] (Sebastian et al. 2016; Trujillo et al. 2020), we set the minimum amplicon depth at 200, 1% substitution errors, 0.001% indel errors, and a 25% minimum dominant frequency. We set the minimum amplicon frequency to 10%.

Our LeasMean MHC sequencing depth per frog was 3433 (range = 82–4776). None of the MHC sequences contained indels or stop codons, suggesting that all alleles were functional. We found no evidence of more than two alleles per individual, suggesting minimal PCR artifacts arising from null alleles or amplifying multiple gene copies.

Amplification of the Cytb gene A 591-bp segment of the cytochrome b mitochondrial gene was amplified with primers 5′-AATGGCCCACACAATACG-3′ and 5′- GTGGATCATACTTGCTGC-3′ based on Bai et al. (2012).[23] The PCRs were conducted in a 25-μL total volume with 10 mm Tris-HCl pH 8.3, 50 mm KCl, 2.5 mm MgCl2, 0.8 μm of each primer, BSA (5 μg), 0.5 U of Taq DNA polymerase (TransGen, Beijing, China) and 20 ng of DNA. The PCR was run with an initial 10-min denaturation step at 95°C; 45 cycles of denaturation at 95°C for 30 s, annealing at 50°C for 40 s and elongation at 72°C for 40 s; followed by a final extension step at 72°C for 5 min. The PCR products were then separated by agarose gel electrophoresis (2% agarose gels). The electrophoretic products were sequenced using the same primers (Beijing Genomics Institute, Beijing, China).

Amplification of Nine Nuclear Microsatellite Loci The nine microsatellites included BF1, BFD11, and GenBank accessions AY323928-AY323933[26] (Table S13). Primer sequences and the procedures for DNA amplification were based on previous works.[56,57] All primers were tagged with 5′-fluorescein bases (TAMRA, FAM or HEX). PCRs were run with conditions of an initial denaturation at 94°C for 3 min followed by 35 cycles of 10 s at 94°C, 30 s at the annealing temperature (Table S2), and 30 s at 72°C and a final 10-min extension at 72°C. The PCR products were separated by 2% agarose gel electrophoresis. We resolved electrophoresis products using an ABI PRISM 377 DNA Sequencer (Applied Biosystems) and scored the microsatellite fragments using GENESCAN version 3.7 (Applied Biosystems) and GeneMarker version 1.71 (SofGenetics).

We quantified the scoring errors resulting from the large allele dropout, stuttering or null alleles using MICRO-CHECKER 2.2.3.[57] We tested the linkage disequilibrium and Hardy-Weinberg equilibrium using GENEPOP version 4.7.5.[58] We found that no microsatellite gene departed from Hardy-Weinberg equilibrium.

Bd DNA extraction and sequencing

Batrachochytrium dendrobatidis DNA was extracted following the procedure of Bai et al. (2012).[28] We amplified Bd DNA using a nested PCR assay with modifications.[28,40] We performed the first amplification using the primers ITS1f and ITS4, which target the conserved regions of the 28S and 18S rRNA genes and

amplify the 5.8S rRNA gene along with the flanking internal transcribed spacer (ITS) of all fungi. The first-round PCR products were then amplified using primers Bd1a and Bd2a with high specificity for Bd.[59] The optimized protocol for PCR amplification involved using 2 μL of each template DNA in a total reaction volume of 25 μL. The PCR mix was composed of 10× PCR buffer (containing 200 mM Tris-HCl, pH 8.4, 200 mM KCl, 100 mM (NH4)2SO4, 20 mM MgSO4, and PCR enhancer), 0.2 mM of each dNTP, 1.25 units of TransStart Taq DNA polymerase (from Beijing TransGen Biotech, Beijing, China), and 0.4 μM of each primer. The conditions for the first amplification included an initial denaturation for 5 min at 94°C; 30 cycles of 30 s at 94°C, 30 s at 59°C and 1 min at 72°C; and a final extension for 10 min at 72°C. The conditions for the second amplification were an initial denaturation for 5 min at 94°C; 30 cycles of 30 s at 94°C, 30 s at 65°C and 30 s at 72°C; and a final extension for 7 min at 72°C. For quality control, sterilized distilled water was used as a negative control, and DNA containing 0.1 Bd zoospore standards were used as a positive control for each amplification.[28] The PCR products, which were approximately 300-bp fragments, were then separated on 2% agarose gels. We tested each sample in triplicate and recorded the sample as Bd positive if two replicates indicated the presence of Bd. Finally, the products from the positive samples were sequenced using the Bd1a and Bd2a primers (Beijing Tianyi Huiyuan Biotechnology Co., LTD).

Metagenomics of pathogenic viruses in environments on islands of the Zhoushan Archipelago

We pelleted each concentrated sample by ultracentrifugation (3 h, 113,000 g, 4°C) and dissolved pelleted particles in 400 μL PBS.[33] Samples were treated with Turbo DNase (Ambion) and RNase (Fermentas) for 60 min at 37°C to digest unprotected nucleic acids, and nucleic acids were extracted with the QIAamp Viral RNA Kit (Qiagen, Netherlands) according to the manufacturer's instructions. Samples were stored at −80°C prior to sequencing.

cDNA synthesis from extracted nucleic acids was performed by sequence-independent RT–PCR amplification[33,60] (Ge et al. 2012; Wang et al. 2017). First strand synthesis was performed using a random primer with murine leukemia virus reverse transcriptase (Promega, WI), and second strand synthesis was performed using Klenow fragment polymerase (Takara, Japan). PCR amplification of second-strand cDNA/DNA was performed using a universal primer based on the oligo employed for primary synthesis using KOD-Plus high-fidelity DNA polymerase (Toyobo, Japan).

Metagenomic sequencing was conducted by Novogene Bioinformatics Technology (Beijing, China). Following DNA purity and concentration measurement, 1 lg of DNA per sample was used for library construction. Library preparations were sequenced on an Illumina HiSeq 4000 platform, and paired-end reads were generated. We removed uncalled bases and screened clean reads for viruses using the GenBank REFSEQ NT (NT=Nucleotide) (version: 2014-10-19) and ACLAME databases.[33] We excluded eukaryotic and bacterial sequences from the datasets. Hits with E-values $<10^{-5}$ were stored for each sequence. Thirty viruses in eight viral families are known to be pathogenic for amphibians (DNA viruses: Iridoviridae, Herpesviridae, Caliciviridae, Flaviviridae, Togaviridae, Adenoviridae; RNA viruses: Caliciviridae and Togaviridae).[61,62] The pathogenic virus diversity or richness in a sample was defined as the number of different pathogenic viruses in the sample, and the abundance of a pathogenic virus was defined as the number of sequences for the virus in the sample. We calculated pathogenic virus diversity and abundance on each island per 40 ml sample.[33] The pathogenic virus diversity or richness in a sample was defined as the number of different pathogenic viruses in the sample, and abundance of a pathogenic virus as number of sequences for the virus in the sample.

Metagenomic sequencing recovered a total of 132,232,676 sequence reads across sites (Table S11), including 43,241,014 sequence reads classified as viral sequences (32.7% of total sequence reads) and 62,663,650 sequence reads associated with no significant similarity to sequences in the GenBank REFSEQ NT and ACLAME databases or with cellular organisms (67.3% of the total sequence reads, including sequences of cellular origin (bacteria, archaea, eukaryote), unclassified sequences, other sequences, unassigned sequences and no hits). The average sequencing depth was approximately equal across sites (10.9–11.3 × 10^6 sequences per location; Table S11).

Statistical analysis

Microsatellites We quantified the expected heterozygosity (He), observed heterozygosity (Ho), and mean number of alleles (Na) for microsatellites across 25 populations using GenAlEx 6.5.[63]

We examined the genetic structure of microsatellites across 25 populations using STRUCTURE 2.3.4.[64] The optimal number of clusters (the best K) was determined using the method of ref.[65] and was implemented in STRUCTURE HARVESTER[66] (Figure S1). Both the admixture model and correlated allele frequency model were simulated. STRUCTURE was run with 10 repetitions of 1,000,000 iterations of MCMC simulation, following a burn-in of 200,000 iterations at K = 1–25.

MHC and cytb We retrieved data on cytb and MHC diversity from LaFond et al. (2022) and downloaded data on cytb and MHC sequences from GenBank (43 cytb haplotypes, GenBank accession numbers: ON457960-ON457993), 28 MHC alleles (ON457936-ON457959) from LaFond et al. (2022),[8] and other MHC alleles (HQ025929-HQ025931; KY587180-KY587181; MN984214 and MN984217 from Mulder t al. 2017 and Trujillo et al. 2021).[34,35]

We calculated nucleotide diversity (π), expected heterozygosity (He), and number of MHC alleles for MHC and nucleotide diversity (π), haplotype diversity (Hd), and number of cytb haplotypes for cytb using DnaSP6 software.[67] We estimated MHC observed heterozygosity (Ho) using Genepop v4.7.5[68] and MHC allelic richness (AR) using FSTAT v2.9.4.[69] We calculated the pairwise population differentiation coefficient (*F*st) of MHC alleles, cytb haplotypes and frequency of microsatellites across 25 populations using Arlequin 3.11.[70]

We compared differences in genetic diversity of MHC, cytb or Bd prevalence among Chinese invasive populations, American invasive and native populations using Mann–Whitney U tests (with significance level $\alpha = 0.05/3 = 0.0167$ after Bonferroni correction). Because no data on microsatellites from American populations are available in GenBank, we only compared the difference in microsatellite diversity between 23 Chinese populations and two US populations in this study using Mann–Whitney U tests.

We identified the relationships among MHC alleles and cytb across 25 populations in this study based on the minimum spanning network. We constructed the networks based on statistical parsimony implemented in TCS in POPART v1.7.[71] We built a phylogenetic tree of all MHC class II sequences and cytb sequences across bullfrog populations in China and America, including the sequences in this study and all available sequences in GenBank. *Xenopus laevis* (accession number: D13688.1) and *Bombina orientalis* (accession number: KJ679330.1) were used as outgroups for the MHC tree, and *Nanorana parkeri* (accession number: NC_026789.1) and *Rana okaloossae* (accession number: AY083284.1) were used as outgroups for cytb[8] (LaFond et al. (2022). We performed sequence alignment using MEGA7 software with the default parameters of ClustalW.[72] We utilized PartitionFinder v2.1.1[73] to determine the optimal model of evolution for the alignment. The best model that was based on the Akaike information criterion corrected for small sample sizes (*AICc*) was HKY + G for MHC and HKY+I+G for cytb. We used MrBayes v3.2.6[74] to reconstruct Bayesian phylogenies. Four chains were run twice for 10 million generations, with the first 100,000 iterations discarded as burn-in. We confirmed Markov chain Monte Carlo convergence and adequate sampling of the posterior distribution (parameter effective sample size >200) using Tracer v1.7[75] to visualize the results.

We identified homologous recombination of MHC alleles using RDP 3.44 with default settings.[76] RDP 3.44 included numerous nonparametric methods for detecting recombination (RDP, GeneConv, BootScan, MaxChi, Chimera, SiScan, PhylPro, LARD, and 3Seq). We identified recombination events as those that were supported by four or more methods.[33]

We identified codon-based positive selection on all MHC sequences in China and the US based on the phylogenetic tree using HyPhy,[77] which is implemented on the Datamonkey server.[78] We used six different methods (FEL, iFEL, SLAC, FUBAR,[78] MEME, and aBSREL) for such analysis, with a significance threshold at $p \leq 0.05$ or a posterior probability ≥ 0.95, depending on the methods. We used MAGA7 to recognize the ABS and non-ABS of the MHC sequences based on the alignment with two sequences (HQ025930 and HQ025931) that were previously checked with that in humans.[79,80] We identified the codons under positive selection if all the methods showed evidence of positive selection (Figure S2 and Table S5).

We grouped supertypes based solely on the functional similarity of their PBR amino acids.[33] We converted an alignment of these amino acid positions into a matrix with five parameters for each amino acid, representing hydrophobicity (z1), steric bulk (z2), polarity (z3), and electronic effects (z4 and z5).[81] We analyzed the matrix using discriminant analysis of principle components (DAPC), as implemented in the R package adegenet 1.4–0.[82] We clustered alleles into distinct groups (supertypes). We determined the optimal

number of clusters by selecting the value with a change in the Bayesian Information Criterion (ΔBIC) of ≤2 (Figure S4).

We investigated the association between MHC alleles and Bd infection by quantifying the relative risk (RR) of Bd infection among all alleles with >5 individuals and Wald confidence intervals using the EpiR package in R.[83] We then performed post hoc Fisher's exact tests on the probability of the RR for each allele.[8]

We examined the relationships between the genetic diversity of MHC, cytb, and microsatellites and environmental pathogenic virus richness and abundance across 13 islands of the Zhoushan Archipelago using Spearman rank correlation.

Phylogenetic tree for Bd haplotypes We downloaded data on Bd haplotypes from GenBank (accession no. FJ232005-FJ232021; FJ010547-FJ229470; EU779859-EU779867; HM153084-HM153085; FJ373880-FJ373885; AY997031; AB435211-AB435231; AB469195-AB469199; JN870740-JN870768; JQ582886-JQ582941).[28,36,40,46] Seven sequences, including two sequences of *Terramyces sp* (AUS3, ITA2590), four *Boothiomyces sp* (AUS8, AUS9, AUS12, ITA2633), and one *Kappamyces sp* (ITA2582), were used as the outgroup, following the methodology by Goka et al. (2009).[40] Phylogenetic relationships among the haplotypes were determined using maximum parsimony, maximum-likelihood, Bayesian inference, and median-joining network methods. We performed maximum parsimony analysis using MEGA5[84] with a heuristic close-neighbor-interchange search[85] and 100 random sequence additions to generate initial trees. All characters were given equal weights, and support for each node was estimated using 10,000 bootstrap analysis replicates. We carried out maximum-likelihood analysis in RAxML v.7.3[86] using the GTR GAMMA model of evolution for tree inference and 10,000 bootstraps.[87] We conducted Bayesian inference using MrBayes v.3.1.2[88] with four chains running for 10 million generations under a GTR+G model of evolution determined by jModelTest v.0.1.1.[89] The burn-in of MCMC chains was assessed using the online program AWTY, examining cumulative plots of posterior probabilities for the 20 most variable splits.[90] We constructed a phylogenetic network to further determine the relationships among worldwide Bd ITS haplotypes using the median-joining method[91] implemented in Network v.4.6.1 (http://www.fluxus-engineering.com).

Statistical analysis

Statistical calculations were carried out using SPSS 19.0. Statistical comparisons between only two groups were carried out by Student's *t* test, but the Mann–Whitney test was used if the data were nonnormally distributed. Statistically significant differences were defined as $p < 0.05$ (*), $p < 0.01$ (**), and $p < 0.001$ (***).

ADDITIONAL RESOURCES

All new genetic sequences generated in this study have been submitted to Genbank (Genank Accession Numbers: OQ606997- OQ607006).